と考えられる[15]。一方で，*SCN5A*の異常はNa^+チャネルの異常を引き起こし，経年的に脱分極異常を惹起する可能性がある。Brugada症候群では，実際にPQ時間，QRS幅やHV時間の延長が報告されており，また遅延電位の陽性率も比較的高く，これらの異常がVFの維持に関与している可能性が考えられる。

4) 治　療

有症候性，すなわちVFが確認されている患者，あるいは安静時の失神発作を有する患者もこれに準ずるが，VF発作の2年以内の再発率が40–50%と高率であり[16]，完全にVFを抑制する抗不整脈薬がない現状では植込み型除細動器(ICD)が必須治療である。補助的治療としてVF発作の頻度を減少させる効果が期待できる経口薬には，I_{to}遮断作用を有するquinidine，I_{Ca}を増強させるdenopamine，atropine，cilostazolなどが挙げられる。VFを頻回に繰り返しているelectrical storm時には，β刺激薬であるisoproterenolの持続点滴やatropineの静注が有効である。

文　献

1) Shimizu W, Antzelevitch C. Sodium channel block with mexiletine is effective in reducing dispersion of repolarization and preventing torsade de pointes in LQT2 and LQT3 models of the long-QT syndrome. Circulation 1997;96:2038–47.
2) Shimizu W, Antzelevitch C. Cellular basis for the electrocardiographic features of the LQT1 form of the long QT syndrome: effects of β-adrenergic agonists, antagonists and sodium channel blockers on transmural dispersion of repolarization and torsade de pointes. Circulation 1998;98:2314–22.
3) Schwartz PJ, Priori SG, Spazzolini C, et al. Genotype–phenotype correlation in the long-QT syndrome: gene-specific triggers for life-threatening arrhythmias. Circulation 2001;103:89–95.
4) Noda T, Takaki H, Kurita T, et al. Gene-specific response of dynamic ventricular repolarization to sympathetic stimulation in LQT1, LQT2 and LQT3 forms of congenital long QT syndrome. Eur Heart J 2002;23:975–83.
5) Shimizu W, Noda T, Takaki H, et al. Diagnostic value of epinephrine test for genotyping LQT1, LQT2 and LQT3 forms of congenital long QT syndrome. Heart Rhythm 2004 (in press)
6) Priori SG, Napolitano C, Schwartz PJ. Low penetrance in the Long-QT syndrome. Clinical impact. Circulation 1999;99:529–33.
7) Shimizu W, Noda T, Takaki H, et al. Epinephrine unmasks latent mutation carriers with LQT1 form of congenital long QT syndrome. J Am Coll Cardiol 2003;41:633–42.
8) Etheridge SP, Compton SJ, Tristani-Firouzi M, et al. A new oral therapy for long QT syndrome: long-term oral potassium improves repolarization in patients with HERG mutations. J Am Coll Cardiol 2003;42:1777–82.
9) Shimizu W, Antzelevitch C. Effects of a K^+ channel opener to reduce transmural dispersion of repolarization and prevent Torsade de Pointes in LQT1, LQT2 and LQT3 models of the long-QT syndrome. Circulation 2000;102:706–12.
10) Brugada P, Brugada J. Right bundle branch block, persistent ST segment elevation and sudden cardiac death: a distinct clinical and electrocardiographic syndrome: a multicenter report. J Am Coll Cardiol 1992;20:1391–6.
11) Di Diego JM, Cordeiro JM, Goodrow RJ, et al. Ionic and cellular basis for the predominance of the Brugada syndrome phenotype in males. Circulation 2002;106:2004–11.
12) Matsuo K, Akahoshi M, Nakashima E, et al. The prevalence, incidence and prognostic value of the Brugada-type electrocardiogram: a population-based study of four decades. J Am Coll Cardiol 2001;38:765–70.
13) Wilde AA, Antzelevitch C, Borggrefe M, et al. Study Group on the Molecular Basis of Arrhythmias of the European Society of Cardiology: Proposed diagnostic criteria for the Brugada syndrome: consensus report. Circulation 2002;106:2514-9.
14) Shimizu W, Matsuo K, Takagi M, et al. Body surface distribution and response to drugs of ST segment elevation in the Brugada syndrome: clinical implication of 87-leads body surface potential mapping and its application to 12-leads electrocardiograms. J Cardiovasc Electrophysiol 2000;11:396–404.
15) Yan GX, Antzelevitch C. Cellular basis for the Brugada syndrome and other mechanisms of arrhythmogenesis associated with ST segment elevation. Circulation 1999;100:1660–6.
16) Kanda M, Shimizu W, Matsuo K, et al. Electrophysiologic characteristics and implication of induced ventricular fibrillation in symptomatic patients with Brugada syndrome. J Am Coll Cardiol 2002; 39:1799–805.

Journal of the American College of Cardiology
© 2005 by the American College of Cardiology Foundation
Published by Elsevier Inc.

Vol. 45, No. 2, 2005
ISSN 0735-1097/05/$30.00
doi:10.1016/j.jacc.2004.09.069

Cellular and Ionic Mechanism for Drug-Induced Long QT Syndrome and Effectiveness of Verapamil

Takeshi Aiba, MD, PHD,* Wataru Shimizu, MD, PHD,† Masashi Inagaki, MD,* Takashi Noda, MD, PHD,* Shunichiro Miyoshi, MD, PHD,‡ Wei-Guang Ding, MD, PHD,§ Dimitar P. Zankov, MD,§‖ Futoshi Toyoda, PHD,§ Hiroshi Matsuura, MD, PHD,§ Minoru Horie, MD, PHD,‖ Kenji Sunagawa, MD, PHD*

Osaka, Tokyo, and Shiga, Japan

OBJECTIVES We examined the cellular and ionic mechanism for QT prolongation and subsequent Torsade de Pointes (TdP) and the effect of verapamil under conditions mimicking *KCNQ1* (I_{Ks} gene) defect linked to acquired long QT syndrome (LQTS).

BACKGROUND Agents with an I_{Kr}-blocking effect often induce marked QT prolongation in patients with acquired LQTS. Previous reports demonstrated a relationship between subclinical mutations in cardiac K^+ channel genes and a risk of drug-induced TdP.

METHODS Transmembrane action potentials from epicardial (EPI), midmyocardial (M), and endocardial (ENDO) cells were simultaneously recorded, together with a transmural electrocardiogram, at a basic cycle length of 2,000 ms in arterially perfused feline left ventricular preparations.

RESULTS The I_{Kr} block (E-4031: 1 μmol/l) under control conditions (n = 5) prolonged the QT interval but neither increased transmural dispersion of repolarization (TDR) nor induced arrhythmias. However, the I_{Kr} blocker under conditions with I_{Ks} suppression by chromanol 293B 10 μmol/l mimicking the *KCNQ1* defect (n = 10) preferentially prolonged action potential duration (APD) in EPI rather than M or ENDO, thereby dramatically increasing the QT interval and TDR. Spontaneous or epinephrine-induced early afterdepolarizations (EADs) were observed in EPI, and subsequent TdP occurred only under both I_{Ks} and I_{Kr} suppression. Verapamil (0.1 to 5.0 μmol/l) dose-dependently abbreviated APD in EPI more than in M and ENDO, thereby significantly decreasing the QT interval, TDR, and suppressing EADs and TdP.

CONCLUSIONS Subclinical I_{Ks} dysfunction could be a risk of drug-induced TdP. Verapamil is effective in decreasing the QT interval and TDR and in suppressing EADs, thus preventing TdP in the model of acquired LQTS. (J Am Coll Cardiol 2005;45:300–7) © 2005 by the American College of Cardiology Foundation

The long QT syndrome (LQTS) is characterized by a prolongation of ventricular repolarization and recurrent episodes of atypical polymorphic ventricular tachycardia known as Torsade de Pointes (TdP) leading to sudden cardiac death (1–3). The molecular basis of congenital LQTS is attributed to defects in several ion channel genes encoding delayed rectifier K^+ or Na^+ currents. On the other hand, agents that block rapidly activating delayed rectifier potassium current (I_{Kr}) often induce marked QT prolongation with an inverted T wave in patients with acquired LQTS. Recent studies indicate that some cases of drug-induced LQTS can be associated with silent mutations and common polymorphism in genes responsible for the congenital LQTS (4), such as *KCNQ1* encoding slowly activating delayed rectifier potassium currents (I_{Ks}) (5–7). However, it remains unclear why subclinical I_{Ks} dysfunction is a risk of drug-induced LQTS.

Both early afterdepolarization (EAD)-induced triggered activity and increased dispersion of repolarization have been suggested as important in the genesis of ventricular arrhythmias in congenital and acquired LQTS. Moreover, verapamil, an L-type Ca^{2+} channel blocker, suppressed EADs and TdP in patients with LQTS (8,9). In the present study, we hypothesized that: 1) addition of I_{Kr} block to I_{Ks} dysfunction markedly prolongs action potential duration (APD) and induces TdP by producing EADs and/or increases transmural dispersion of repolarization (TDR); and 2) verapamil suppresses TdP by preventing EADs and decreasing TDR. In arterially perfused feline left ventricular wedge preparations, we demonstrated that subclinical I_{Ks} dysfunction, mimicking *KCNQ1* defect, could be a risk of drug-induced TdP, and verapamil successfully suppressed TdP in the model of acquired LQTS.

METHODS

Arterially perfused wedge preparations and electrophysiologic recordings. All animal care procedures were in accordance with the position of the American Heart Association research animal use (November 11, 1984). The

From the *Department of Cardiovascular Dynamics, Research Institute, and †Division of Cardiology, Department of Internal Medicine, National Cardiovascular Center, Suita, Osaka, Japan; the ‡Department of Physiology, Keio University School of Medicine, Tokyo, Japan; §Department of Physiology and ‖Department of Cardiovascular and Respiratory Medicine, Shiga University of Medical Science, Otsu, Shiga, Japan. This study was supported by the Program for Promotion of Fundamental Studies in Health Science of the Organization for Pharmaceutical Safety and Research (of Japan) (to Dr. Sunagawa), a grant from the Japan Cardiovascular Research Foundation (to Dr. Aiba), Fukuda Foundation for Medical Technology (to Dr. Inagaki), Vehicle Racing Commemorative Foundation (to Dr. Shimizu), Health Sciences Research Grants from the Ministry of Health, Labour and Welfare (to Dr. Shimizu), and the Research grant for Cardiovascular Disease (15C-6) from the Ministry of Health, Labour and Welfare (to Dr. Shimizu).

Manuscript received August 24, 2004; revised manuscript received September 21, 2004, accepted September 28, 2004.

Abbreviations and Acronyms

APD_{90} = action potential duration measured at 90% repolarization
BCL = basic cycle length
EAD = early afterdepolarization
I_K = delayed rectifier potassium current
I_{Kr} = rapidly activating delayed rectifier potassium current
I_{Ks} = slowly activating delayed rectifier potassium current
LQTS = long QT syndrome
TdP = Torsade de Pointes
TDR = transmural dispersion of repolarization

methods used for isolation, perfusion, and recording of transmembrane activity from the arterially perfused feline left ventricle have been detailed in a previous study (10) and are similar to methods reported using canine or rabbit wedge preparations (11–15). Briefly, a transmural wedge was dissected from the anterior wall of the left ventricle, cannulated via the left descending coronary artery (or the first branch of the left circumflex), and placed in a small tissue bath arterially perfused with Tyrode's solution. The temperature was maintained at 37 ± 1°C and perfusion pressure maintained between 40 and 60 mm Hg. Ventricular wedges were stimulated with bipolar electrodes applied to the endocardial surface. We recorded a transmural electrocardiogram (ECG) (epicardial, positive pole) using Ag-AgCl electrodes, and transmembrane action potentials (APs) simultaneously from the epicardium, midmyocardium (M), and endomyocardium using three separate intracellular floating microelectrodes. The epicardial and endocardial APs were recorded from the epicardial and endocardial surfaces, respectively, at positions approximating the transmural axis of the ECG. The M-cell's AP was recorded from the transmural surface, mainly at the subendocardium, along the same axis.

An I_{Kr} blocker, E-4031 1 μmol/l, was used in control condition (n = 5) or under condition with I_{Ks} suppression by chromanol 293B 10 μmol/l, mimicking *KCNQ1* defect (n = 10). The effects of an L-type Ca^{2+} channel blocker, verapamil, were evaluated at 0.1, 1, 2.5, and 5 μmol/l under the I_{Ks} and I_{Kr} suppression (acquired LQTS condition). Epinephrine 0.5 μmol/l was used to mimic increased sympathetic activity in the absence and presence of verapamil under the acquired LQTS condition. The spontaneous or epinephrine-induced EADs and subsequent TdP were evaluated under each set of conditions.

Data using E-4031, 293B, 293B + E-4031, and additional verapamil on top of 293B + E-4031 were collected for a period of 30 min starting 30 min after applying the above compounds to the perfusion. The APD was measured at 90% repolarization (APD_{90}). The TDR was defined as the difference between the longest and shortest repolarization times (activation time + APD_{90}) of the APs recorded across the wall. The QT interval was defined as the time interval between the QRS onset and the point at which the line of maximal downslope of the positive T wave and the line of the maximal upslope of the negative T wave crossed the baseline.

Whole-cell patch-clamp experiments. Epicardial, M, and endocardial cells isolated from the feline left ventricle were voltage-clamped using whole-cell configuration of the patch-clamp technique (16). Patch electrodes were pulled from borosilicate glass capillaries, heat-polished, and had a tip resistance of 2.0 to 3.0 MΩ when filled with standard pipette solution containing (mmol/l): 70 potassium aspartate, 50 KCl, 10 KH_2PO_4, 1 $MgSO_4$, 3 Na_2-ATP, 0.1 Li_2-GTP, 5 EGTA, and 5 HEPES (pH adjusted to 7.2 with KOH). Membrane currents were recorded from the epicardial, M, and endocardial cells superfused at 34 to 36°C with normal Tyrode's solution containing (mmol/l): 140 NaCl, 5.4 KCl, 1.8 $CaCl_2$, 0.5 $MgCl_2$, 0.33 NaH_2PO_4, 5.5 glucose, and 5.0 HEPES (pH adjusted to 7.4 with NaOH). In all current measurements, nisoldipine (0.4 μmol/l) was added to normal Tyrode's solution to abolish $I_{Ca,L}$. The cell membrane capacitance (C_m) was calculated for each cell by fitting the single exponential function to the decay of the capacitive transient elicited by a 5-mV step hyperpolarization applied from a holding potential of −50 mV (17).

Simulation study. Isolated epicardial, M, and endocardial cells were simulated using a Luo-Rudy dynamic cell model modified by varying the maximum conductance (density) of I_{Kr} and I_{Ks} (G_{Kr} and G_{Ks}) as described previously (18), in which the G_{Ks}/G_{Kr} in the epicardial, M, and endocardial cells were 23, 17, and 19, respectively. The transient outward potassium current (I_{to}) was incorporated into the model using the formulation of Dumaine et al. (19), in which the maximum conductance of I_{to} (G_{to}) was set to 0.5, 0.25, and 0.05 mS/μF in the epicardial, M, and endocardial cells, respectively.

Statistics. Statistical analysis of the data was performed with a Student *t* test for paired data or analysis of variance coupled with Bonferroni's test, as appropriate. Data are expressed as mean values ± SD except for those shown in the figures, which are expressed as mean ± SEM. Significance was defined as a value of $p < 0.05$.

RESULTS

The QT interval, APD, and TDR under an acquired LQTS condition with or without epinephrine. Figure 1 shows transmembrane activity recorded simultaneously from the epicardium, M, and endocardium together with a transmural ECG at a basic cycle length (BCL) of 2,000 ms. E-4031 (1 μmol/l) alone significantly, but homogenously, prolonged APD of the three regions, causing no major change in TDR (Fig. 1B). Chromanol 293B (10 μmol/l) alone did not significantly increase the QT interval, APD of the three regions, and TDR (Fig. 1C). The additional E-4031 to 293B, mimicking acquired LQTS, preferentially prolonged epicardial APD, thus dramatically increased QT

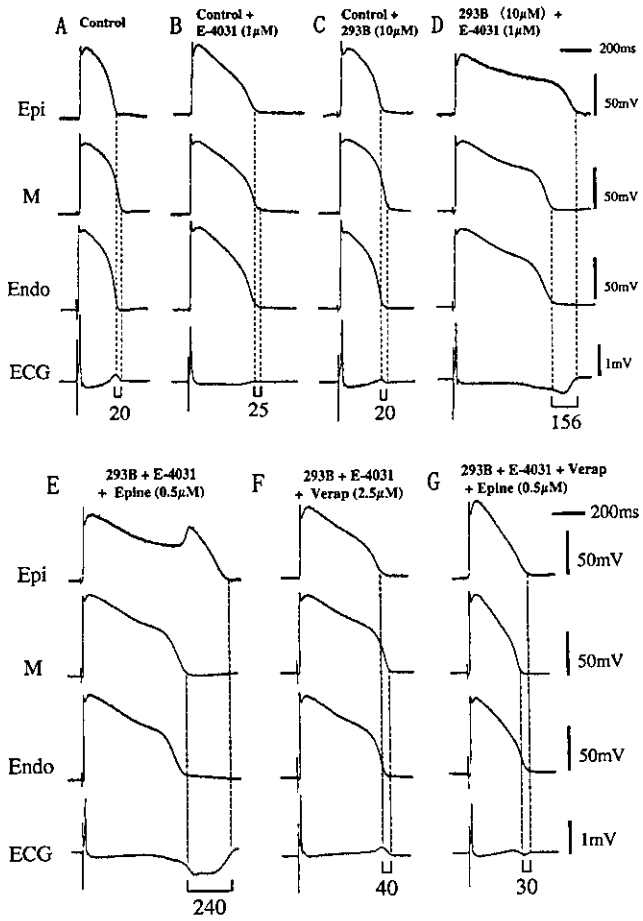

Figure 1. Transmembrane action potentials simultaneously recorded from the epicardial (Epi), midmyocardial (M), and endocardial (Endo) regions and a transmural electrocardiogram (ECG) at basic cycle length of 2,000 ms under each study condition. **(A)** Control. **(B)** E-4031 (1μmol/l). **(C)** Chromanol 293B (10μmol/l). **(D)** 293B + E-4031 (acquired long QT syndrome [LQTS] condition). **(E)** Epinephrine infusion (Epine: 0.5μmol/l) under acquired LQTS condition. **(F)** Addition of verapamil (Verap) 2.5 μmol/l under acquired LQTS condition. **(G)** Further addition of Epine in the continued presence of Verap under acquired LQTS condition. Numbers at bottom of each ECG denote transmural dispersion of repolarization (ms).

interval and TDR (Fig. 1D). Epinephrine infusion (0.5 μmol/l) further prolonged epicardial APD associated with induction of EADs, but did not prolong M or endocardial APD, resulting in further QT prolongation and increasing TDR (Fig. 1E).

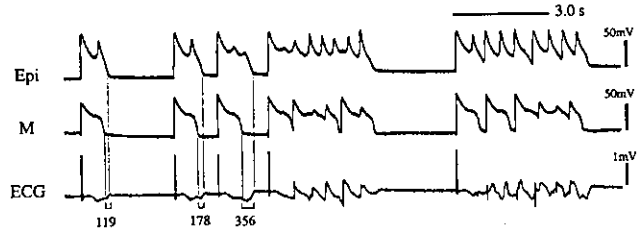

Figure 2. Spontaneous early afterdepolarization and subsequent Torsade de Pointes under the acquired long QT syndrome condition (293B 10 μmol/l + E-4031 1 μmol/l). Basic cycle length = 3,000 ms. Recordings and abbreviations as in Figure 1.

The composite data of the QT interval, APD_{90} of the epicardium, M, and endocardium, and TDR at a BCL of 2,000 ms are shown in Table 1. E-4031 under control significantly, but homogeneously, prolonged APD_{90}, resulting in neither change of TDR nor induction of arrhythmia. Chromanol 293B under control did not significantly increase APD_{90} of the three regions, resulting in no major change in QT interval and TDR. Whereas additional E-4031 to 293B markedly prolonged QT interval as evidenced by preferential prolongation of the epicardial APD_{90} compared with M and endocardial APD_{90}, thus dramatically increased TDR. Epinephrine further prolonged the epicardial APD_{90}, but shortened the M region APD_{90}, resulting in further prolongation of the QT interval and increasing TDR.

Neither E-4031 alone nor 293B alone produced any EADs or TdP. However, additional E-4031 to 293B (acquired LQTS condition) induced spontaneous EADs from the epicardium in 5 of 10 preparations, including two preparations with spontaneous TdP (Fig. 2), but not from the M or endocardium. Further epinephrine infusion (n = 8) induced EADs from the epicardium in all preparations, including four preparations with subsequent TdP, but EADs from the M region were seen in only one preparation.

Effect of verapamil on the QT interval, APD, TDR, and induction of arrhythmias under an acquired LQTS condition. Under the acquired LQTS condition, verapamil dose-dependently (0.1 to 5 μmol/l) abbreviated APD of

Table 1. Effect of I_{Kr} Block With or Without Pretreated I_{Ks} Block on the QT Interval, APD_{90}, and Transmural Dispersion of Repolarization

		APD_{90}			
	QT	Epi	M	Endo	TDR
Control (n = 5)	283 ± 15	227 ± 16	259 ± 8	246 ± 13	31 ± 10
E-4031 (1 μM) (n = 5)	446 ± 42*	373 ± 30*	408 ± 28*	374 ± 25*	34 ± 4
Control (n = 10)	279 ± 12	230 ± 16	253 ± 14	237 ± 19	24 ± 5
293B (10 μM) (n = 10)	298 ± 34	252 ± 26	275 ± 33	253 ± 16	24 ± 9
293B (10 μM) + E-4031 (1 μM) (n = 10)	793 ± 183*	723 ± 164*	596 ± 131*	545 ± 78*	175 ± 68*
293B + E-4031 + Epine (0.5 μM) (n = 8)	866 ± 251	801 ± 217	506 ± 123	525 ± 118	191 ± 75
293B + E-4031 + Verap (2.5 μM) (n = 7)	557 ± 178‡	503 ± 171‡	483 ± 135†	516 ± 154	35 ± 37‡
293B + E-4031 + Verap + Epine (n = 6)	445 ± 113‡	403 ± 117‡	399 ± 93‡	411 ± 98†	30 ± 12‡

*$p < 0.001$ vs. control, †$p < 0.05$ vs. 293B + E-4031; ‡$p < 0.01$ vs. 293B + E-4031 by analysis of variance with Bonferroni's test.
APD_{90} = action potential duration at 90% repolarization; Endo = endocardium; Epi = epicardium; Epine = epinephrine; I_{Ks} = slowly activating delayed rectifier potassium current; I_{Kr} = rapidly activating delayed rectifier potassium current; M = mid-myocardium; QT = QT interval; TDR = transmural dispersion of repolarization; Verap = verapamil.

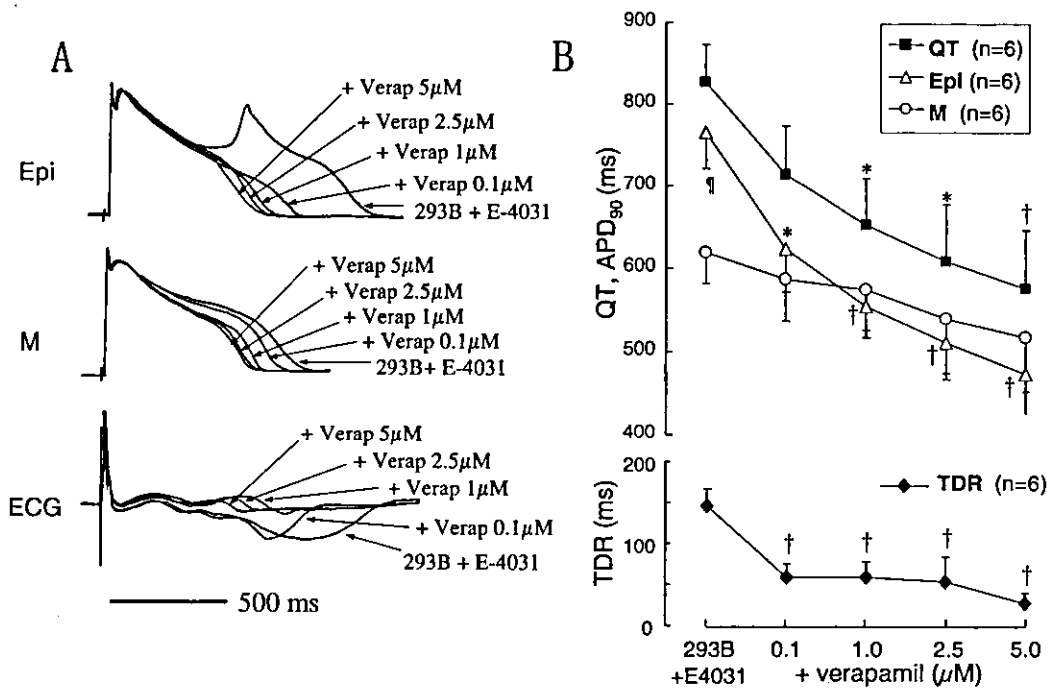

Figure 3. Dose-dependent effect of Verap (0.1 to 5 μmol/l) on transmembrane and ECG activity under acquired LQTS condition (293B 10 μmol/l + E-4031 1 μmol/l). **(A)** Superimposed action potentials recorded simultaneously from the epicardial and M regions together with a transmural ECG. **(B)** Composite data of the effect of Verap on QT interval **(solid squares)**, action potential duration measured at 90% repolarization (APD_{90}) of Epi **(open triangles)** and M **(open circles)** regions and transmural dispersion of repolarization (TDR) **(solid diamonds)**. Basic cycle length = 2,000 ms. *$p < 0.05$ vs. 293B + E-4031; †$p < 0.01$ vs. 293B + E-4031; ¶$p < 0.05$ vs. M region by analysis of variance with Bonferroni's test. Abbreviations as in Figure 1.

the epicardial and M regions as well as the QT interval (Fig. 3A). Figure 3B shows composite data of the dose-dependent effect of verapamil on the QT interval, APD_{90} of the epicardial and M regions, and TDR under the acquired LQTS condition (n = 6). A 5-μmol/l dose of verapamil under the acquired LQTS condition preferentially abbreviated the epicardial APD_{90} (761 ± 99 ms to 469 ± 95 ms; $p < 0.001$) compared with the M region APD_{90} (615 ± 83 ms to 512 ± 146 ms; p = NS), resulting in a significant decrease in TDR (146 ± 46 ms to 26 ± 28 ms; $p < 0.01$). The change in QT interval paralleled the decrease in the epicardial APD_{90}.

As shown in Figure 1F, 2.5-μmol/l verapamil preferentially abbreviated the epicardial APD_{90} rather than the M or endocardium, thus significantly abbreviated QT interval and TDR. Moreover, verapamil completely prevented the influence of epinephrine in inducing EADs and TdP as well as increasing the epicardial APD_{90}, QT interval, and TDR (Fig. 1G). The composite data of the effect of verapamil on the QT interval, APD, and TDR with or without epinephrine are shown in Table 1. Thus, verapamil totally suppressed EADs and TdP under the acquired LQTS condition with or without epinephrine.

Measurement of I_{Kr} and I_{Ks} in epicardial, M, and endocardial cells. Figure 4A represents the dose-dependent inhibition of I_{Ks} by 293B in an epicardial cell. Figure 4B illustrates the concentration-response relationships for the inhibition of I_{Ks} tail current. The data points were reasonably well described by a Hill equation with the following parameters: IC_{50} = 6.39 ± 1.17 μmol/l, n_H = 1.23 ± 0.05 (epicardial cells: n = 5); IC_{50} = 5.71 ± 1.32 μmol/l, n_H = 1.25 ± 0.12 (M cells: n = 5); IC_{50} = 5.73 ± 0.94 μmol/l, n_H = 1.07 ± 0.19 (endocardial cells: n = 5). There are no significant differences in IC_{50} and n_H values among the epicardial, M, and endocardial cells (analysis of variance with Bonferroni's test), thus indicating that I_{Ks} in these three cell types represents a similar sensitivity to inhibition by chromanol 293B.

Figure 5 represents the sensitivity of I_K to blockers of I_{Kr} and I_{Ks} (E-4031 and 293B, respectively). After the I_K reached a practically steady level (control, trace 1), application of E-4031 (3 μmol/l) markedly reduced the amplitude of I_K tail current (trace 2), and further addition of 293B (30 μmol/l) almost completely abolished the I_K tail current (trace 3). Table 2 summarizes densities of I_{Kr} and I_{Ks} in the epicardial, M, and endocardial cells, determined as E-4031- and 293B-sensitive tail currents normalized with reference to C_m. In each cell type, the density of I_{Ks} was significantly smaller than that of I_{Kr}. The density of I_{Kr} was almost equivalent among the three cell types, whereas I_{Ks} density was significantly smaller in M cells compared with that in the epicardial and endocardial cells.

Computer simulations. To understand why EAD developed from the epicardium under the acquired LQTS

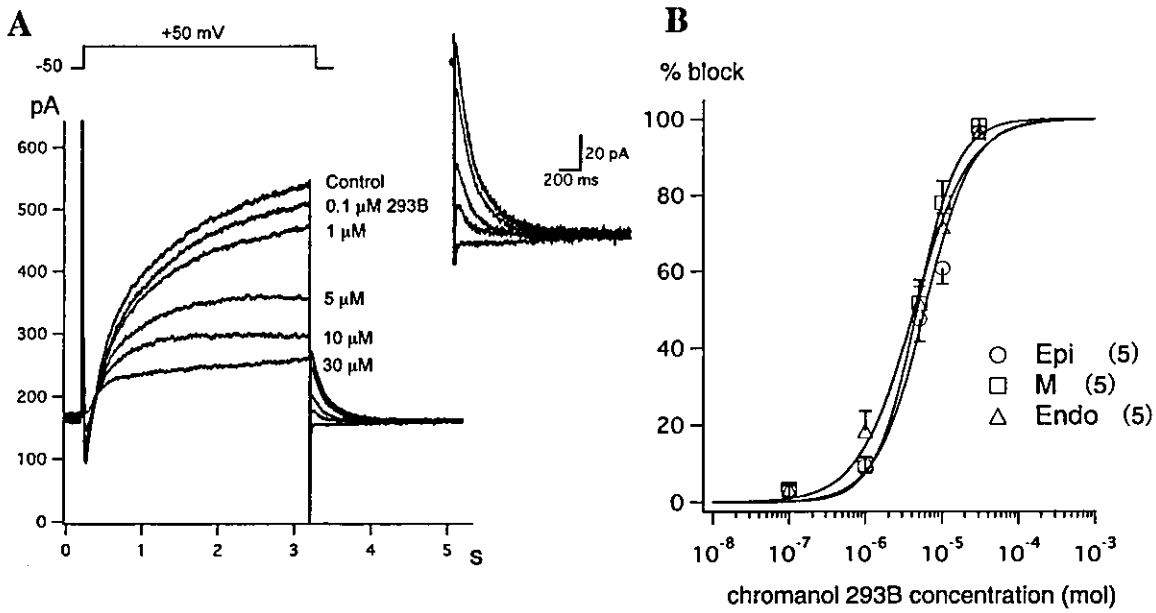

Figure 4. Sensitivity of I_{Ks} in the epicardial (Epi), midmyocardial (M), and endocardial (Endo) cells to inhibition by chromanol 293B. **(A)** Representative superimposed current traces elicited by 3-s depolarizing voltage-clamp steps applied from a holding potential of −50 mV to +50 mV in an epicardial cell, before (control) and during exposure to 293B at a concentration of 0.1, 1, 5, 10, and 30 μmol/l. The I_{Kr} inhibitor E-4031 (3 μmol/l) was present throughout. Tail currents were demonstrated on an expanded scale. **(B)** The percent block of I_{Ks} in the Epi **(open circles)**, M **(open squares)**, and Endo **(open triangles)** cells. The degree of I_{Ks} inhibition was measured as the fraction of the tail current reduced by each concentration of 293B with reference to the control amplitude of the tail current. **Smooth curves** through the data points represent a least-squares fit of a Hill equation: percent block = $100/(1 + (IC_{50}/[293B])^{nH})$, yielding the concentration required for the half-maximal block (IC_{50}) and the Hill coefficient (n_H). pA = pico (× 10^{-12}) Ampere.

condition, we simulated APs of the three cell types using a Luo-Rudy model at a BCL of 2,000 ms. As shown in Figure 6A, the epicardial APD was shorter than the M cells under the control condition (dotted line). However, suppression of both I_{Kr} and I_{Ks} (70% and 80%, respectively) (solid line), simulating the condition of acquired LQTS, developed EAD (arrow) from the epicardial cell but not from M or endocardial cells. Moreover, Figure 6B shows that the reactivation of Ca^{2+} current through the L-type channel ($I_{Ca,L}$) was responsible for the development of epicardial EAD under the acquired LQTS condition. Furthermore, a decrease in I_{to} density changed by G_{to} from 0.5 to 0.05

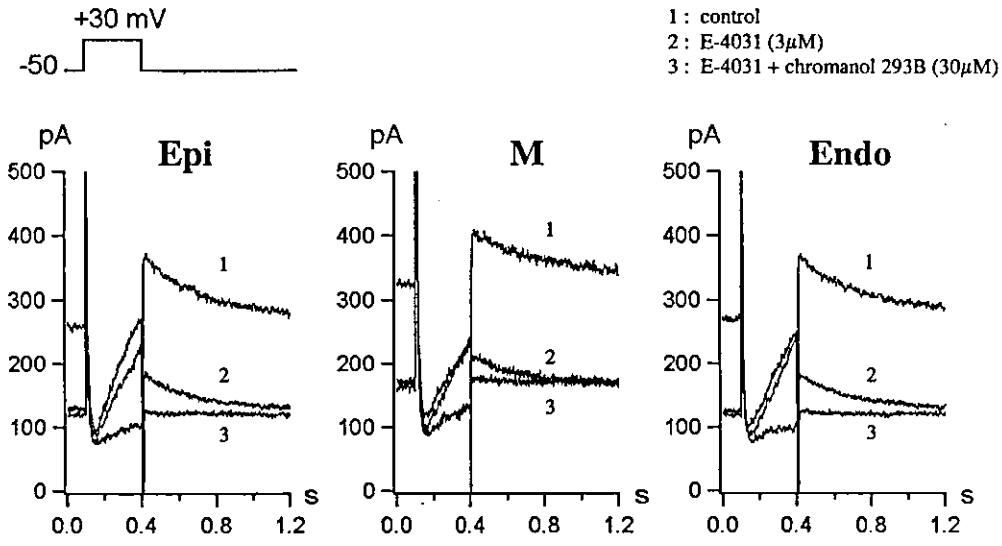

Figure 5. Detection of I_{Kr} and I_{Ks} in the epicardial (Epi), midmyocardial (M), and endocardial (Endo) cells. Depolarizing test pulses (to +30 mV for 300 ms) were repetitively applied (every 2 s) from a holding potential of −50 mV to activate I_K, and membrane currents were recorded from the Epi, M, and Endo cells, before (trace 1), and ~2 min after exposure to 3 μmol/l E-4031 (trace 2), and ~2 min after further addition of 30 μmol/l 293B in conjunction with 3 μmol/l E-4031 (trace 3). pA = pico (× 10^{-12}) Ampere.

Table 2. Transmural Heterogeneity of I_{Ks} and I_{Kr} in Feline Left Ventricle

	Epi (n = 10)	M (n = 9)	Endo (n = 7)
I_{Ks}	0.35 ± 0.26*	0.13 ± 0.09*†	0.30 ± 0.09*
I_{Kr}	1.34 ± 0.51	1.10 ± 0.38	1.17 ± 0.30

*$p < 0.05$ vs. I_{Ks}; †$p < 0.05$ vs. Epi and Endo by analysis of variance with Bonferroni's test. Mean ± SD, (pA/pF). Current densities of I_{Kr} and I_{Ks} measured as E-4031- and chromanol 293B-sensitive tail currents at −50 mV.
Abbreviations as in Table 1.

mS/μF decreased the net charge entry carried by the $I_{Ca,L}$ during the AP, resulted in suppressing EAD as well as abbreviating APD.

DISCUSSION

Genetic and ionic substrates of acquired LQTS. Acquired QT prolongation and TdP arrhythmias usually require multiple risk factors, such as bradycardia, hypokalemia, female gender, and mostly agents with an I_{Kr}-blocking effect. Recent genetic studies suggest some forms of acquired LQTS can be associated with silent mutations in the LQTS-related genes (4), such as *KCNQ1* encoding I_{Ks} (so-called forme fruste type of congenital LQTS) (5–7). Roden (20) hypothesized "reduced repolarization reserve" as a potential mechanism underlying susceptibility to drug-induced LQTS. According to his hypothesis, I_{Ks} dysfunction could be potentially compensated by other K^+ currents, mainly I_{Kr}, thereby the repolarization defect is tolerated, and agents with I_{Kr} block could induce acquired QT prolongation and TdP.

Vos et al. (21–23) suggested a high incidence of EADs and TdP by *d*-sotalol in dogs with chronic complete atrioventricular block as a result of a significant down-regulation of I_{Ks} and I_{Kr}. Moreover, other experimental studies using canine and rabbit wedge showed combined I_{Ks} and I_{Kr} block caused a high incidence of EADs most likely arising from the epicardium (14,15). Burashnikov and Antzelevitch (24) suggested that the abundant I_{Ks} in the epicardium and endocardium compared with the M region under normal conditions contributed to the increase in TDR but protected against development of EADs in the epicardium and endocardium in dogs. Thus, I_{Ks} is critically important for the repolarization reserve in the epicardium and endocardium.

Although I_{Ks} in the feline heart is far smaller than that in other species (25,26), our result from a whole-cell patch-clamp study suggested that a 10-μmol/l 293B used in the wedge preparation reduced about 70% of I_{Ks} in the three cell types, which is consistent with degree of I_{Ks} blockade caused by a silent mutation or common polymorphism in human *KCNQ1* gene (6,7). We also showed that I_{Kr} block with E-4031 in control conditions prolonged the QT interval but did not increase TDR and developed neither EADs nor TdP. However, combined I_{Kr} block with 293B further prolonged the QT interval and inverted T wave, which, in turn, increased TDR and induced EADs and TdP. There-

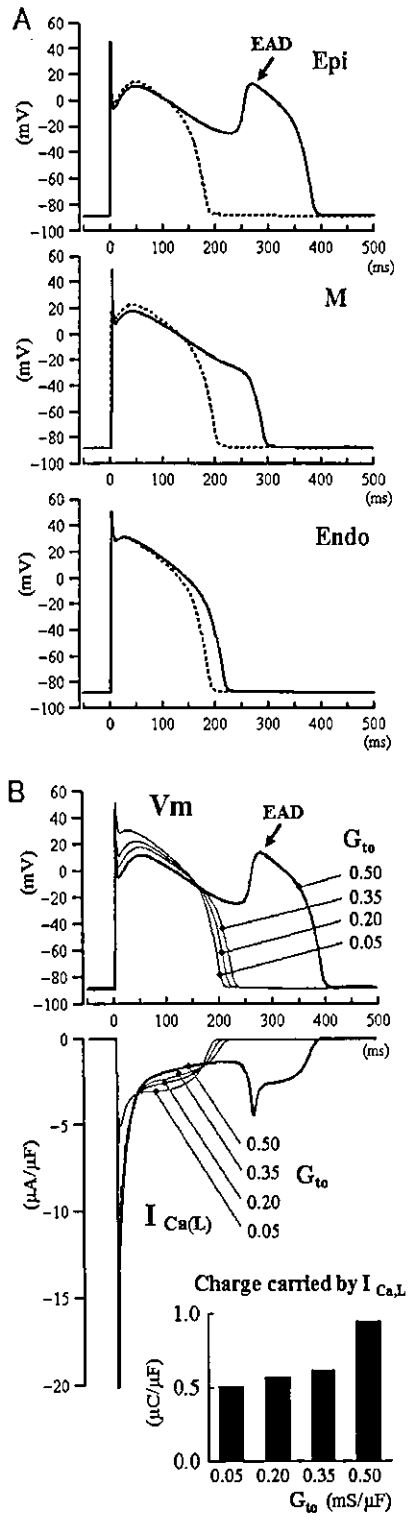

Figure 6. Effect of both I_{Kr} and I_{Ks} suppression on the simulated action potentials from the epicardial (Epi), midmyocardial (M), and endocardial (Endo) cells. **(A)** Superimposed action potentials simulated under baseline condition **(dotted lines)** and after both I_{Kr} and I_{Ks} suppression (70% and 80%, respectively) **(solid lines)**. **(B)** Effect of maximum conductance of I_{to} (G_{to}) on the simulated epicardial action potential (Vm), $I_{Ca,L}$ magnitude, and the net charge entry calculated by integration of the $I_{Ca,L}$ under the condition of both I_{Kr} and I_{Ks} suppression. Basic cycle length = 2,000 ms. EAD = early afterdepolarization.

fore, the feline heart is appropriate for a model of forme fruste LQTS. Our data also suggested that subclinical I_{Ks} dysfunction may become a genetic substrate, and additional I_{Kr} suppression may unmask marked QT prolongation and TdP in acquired form of LQTS.

Role of $I_{Ca,L}$ in increasing TDR and inducing EADs and TdP in acquired LQTS. Several clinical and experimental studies have suggested that EADs and triggered activity were important in the genesis of QT prolongation and TdP in LQTS (8,9,11–15,22–24). Induction of EADs generally requires an initiation or conditioning phase controlled by the sum of membrane currents present at the plateau AP (inward depolarization current and outward repolarization current). January and Riddle (27) suggested that the time- and voltage-dependent $I_{Ca,L}$ within its "window" was important in the induction and block of EADs. Luo and Rudy (28) suggested that EADs resulted from a secondary activation of the $I_{Ca,L}$ during the plateau of AP. However, the mechanism responsible for a high incidence of EADs (especially from the epicardium) and subsequent TdP under conditions of severely eliminated outward K^+ current, mimicking acquired LQTS, has not been mechanistically defined.

Our data indicate that accentuation of $I_{Ca,L}$ during the AP plateau preferentially prolonged APD and triggered EADs in the epicardium. This was based on the effect of verapamil on the epicardium. However, it is still unclear whether a larger $I_{Ca,L}$ in the epicardial cell compared with the M or endocardial cells contributed to the development of EADs. Recently, Bányász et al. (29) reported in their AP voltage clamp experiments that the epicardial cell had a pool of Ca^{2+} channels sufficient for a second activation, whereas the endocardial cells did not. Cordeiro et al. (30) also noted that the presence of spike-and-dome AP waveform in the epicardial cells resulted in a greater magnitude of $I_{Ca,L}$. Moreover, several simulation studies demonstrated a strong coupling between $I_{Ca,L}$ and I_{to} (31,32). Our simulation study also suggested that larger I_{to} in the epicardial cell caused larger $I_{Ca,L}$, developing EADs under the acquired LQTS condition. In the feline left ventricle, it has been reported that I_{to} is larger in the epicardium compared with the endocardium (33). Therefore, larger $I_{Ca,L}$ secondary to I_{to}-mediated spike-and-dome AP configuration in the epicardial cell might be responsible for the high incidence of EADs from the epicardium. This does not necessarily exclude the possible mechanisms of other ionic currents such as I_{NaCa} and Ca^{2+} release from sarcoplasmic reticulum, which may contribute to the prolonged AP as well as to the development of EADs under calcium-loading conditions (34).

Effects of catecholamines and verapamil in acquired LQTS. Treatment of drug-induced TdP begins with immediate withdrawal of any potential drugs and risk factors. Sanguinetti et al. (35) suggested that an increase of heart rate by isoproterenol was an effective therapeutic strategy in patients with acquired LQTS, because beta-adrenergic stimulation with isoproterenol abbreviates repolarization not only by increasing heart rate, but also by directly increasing the magnitude of I_{Ks}. However, our experimental data shows that epinephrine further prolonged APD in the epicardium and induced EADs and TdP probably due to augmentation of $I_{Ca,L}$ in the acquired LQTS condition. Thus, beta-adrenergic stimulation could be arrhythmogenic even in conditions of acquired LQTS when subclinical I_{Ks} dysfunction is present and heart rate is not fully increased.

Cosio et al. (8) used intravenous verapamil to treat three patients with TdP during an atrioventricular block. Shimizu et al. (9) reported that verapamil suppressed spontaneous or epinephrine-induced EADs and TdP in patients with congenital LQTS. Experimentally, Kimura et al. (36) reported that verapamil (2 μmol/l) suppressed cocaine-induced EADs in the myocytes isolated from feline left ventricle. Taken together with the data in the present study, $I_{Ca,L}$ block with verapamil may be a therapeutic choice for TdP in patients with acquired LQTS as well as congenital LQTS.

Study limitations. We assumed the activity recorded from the cut surface of the perfused wedge preparation represented cells within the respective layers of the wall throughout the wedge. Such validation was provided in previous studies that used the wedge preparation (10–15).

Pharmacologic block of I_{Ks} with 293B is not a complete surrogate for *KCNQ1* defect. However, our feline model closely mimicked the degree of I_{Ks} inhibition and pharmacologic features of acquired LQTS. Therefore, we believe these qualitative similarities validate 293B as a surrogate for forme fruste LQTS.

We simulated APs of the three cell types using a Luo-Rudy model, but it does not completely represent feline ventricular APs. However, the phenomenon that EAD frequently developed from the epicardium under the acquired LQTS condition was observed not only in cats but also in dogs and rabbits (14,15); thus, this simulation may support our speculation about the mechanism of this phenomenon.

Finally, the concentration of verapamil mainly used in this study (2.5 μmol/l = 1,250 ng/ml) was considerably higher than a typical clinical dose. However, verapamil was effective in suppressing EADs and decreasing TDR even at the lowest dose used in this study (0.1 μmol/l = 50 ng/ml), which is close to plasma concentration of verapamil after a 5-mg bolus injection (below 200 ng/ml).

Acknowledgments

The authors thank Drs. Charles Antzelevitch and Masahiko Kondo for their helpful suggestions and technical instructions, and Drs. Hans-J. Lang and Jürgen Pünter (Aventis Pharma Deutschland GmbH, Frankfurt, Germany) for kindly providing the chromanol 293B.

Reprint requests and correspondence: Dr. Wataru Shimizu, Division of Cardiology, Department of Internal Medicine, National Cardiovascular Center, 5-7-1 Fujishiro-dai, Suita, Osaka, 565-8565 Japan. E-mail: wshimizu@hsp.ncvc.go.jp.

REFERENCES

1. Schwartz PJ, Periti M, Malliani A. The long Q-T syndrome. Am Heart J 1975;89:378–90.
2. Moss AJ, Schwartz PJ, Crampton RS, et al. The long QT syndrome: prospective longitudinal study of 328 families. Circulation 1991;84: 1136–44.
3. Roden DM, Lazzara R, Rosen M, et al. Multiple mechanisms in the long-QT syndrome: current knowledge, gaps and future directions. Circulation 1996;94:1996–2012.
4. Yang P, Kanki H, Drolet B, et al. Allelic variants in long-QT disease genes in patients with drug-associated Torsades de Pointes. Circulation 2002;105:1943–8.
5. Donger C, Denjoy I, Berthet M, et al. KVLQT1 c-terminal missense mutation causes a forme fruste long-QT syndrome. Circulation 1997;96:2778–81.
6. Napolitano C, Schwartz PJ, Brown AM, et al. Evidence for a cardiac ion channel mutation underlying drug-induced QT prolongation and life-threatening arrhythmias. J Cardiovasc Electrophysiol 2000;11: 691–6.
7. Kubota T, Shimizu W, Kamakura S, et al. Hypokalemia-induced long QT syndrome with underlying novel missense mutation in S4-S5 linker of KCNQ1. J Cardiovasc Electrophysiol 2000;11:1048–54.
8. Cosio FG, Goicolea A, López-Gil L, Kallmeter C, Barroso L. Suppression of Torsades de Pointes with verapamil in patients with atrio-ventricular block. Eur Heart J 1991;12:635–8.
9. Shimizu W, Ohe T, Kurita T, et al. Effects of verapamil and propranolol on early afterdepolarizations and ventricular arrhythmias induced by epinephrine in congenital long QT syndrome. J Am Coll Cardiol 1995;26:1299–309.
10. Aiba T, Shimizu W, Inagaki M, et al. Transmural heterogeneity of the action potential configuration in the feline left ventricle. Circ J 2003;67:449–54.
11. Antzelevitch C, Sun ZQ, Zhang ZQ, Yan GX. Cellular and ionic mechanisms underlying erythromycin-induced long QT intervals and Torsade de Pointes. J Am Coll Cardiol 1996;28:1836–48.
12. Shimizu W, Antzelevitch C. Sodium channel block with mexiletine is effective in reducing transmural dispersion of repolarization and preventing Torsade de Pointes in LQT2 and LQT3 models of the long-QT syndrome. Circulation 1997;96:2038–47.
13. Shimizu W, Antzelevitch C. Effects of a K^+ channel opener to reduce transmural dispersion of repolarization and prevent Torsade de Pointes in LQT1, LQT2, and LQT3 models of the long-QT syndrome. Circulation 2000;102:706–12.
14. Emori T, Antzelevitch C. Cellular basis for complex T wave and arrhythmic activity following combined I_{Kr} and I_{Ks} block. J Cardiovasc Electrophysiol 2001;12:1369–78.
15. Yan GX, Wu Y, Liu T, et al. Phase 2 early afterdepolarization as a trigger of polymorphic ventricular tachycardia in acquired long-QT syndrome, direct evidence from intracellular recordings in the intact left ventricular wall. Circulation 2001;103:2851–6.
16. Hamill OP, Marty A, Neher E, Sakmann B, Sigworth FJ. Improved patch-clamp techniques for high-resolution current recording from cells and cell-free membrane patches. Pflügers Arch 1981;391:85–100.
17. Benitah JP, Gomez AM, Bailly P, et al. Heterogeneity of the early outward current in ventricular cells isolated from normal and hypertrophied rat hearts. J Physiol 1993;469:111–38.
18. Clancy CE, Rudy Y. Na^+ channel mutation that causes both Brugada and long-QT syndrome phenotypes, a simulation study of mechanism. Circulation 2002;105:1208–13.
19. Dumaine R, Towbin JA, Brugada P, et al. Ionic mechanisms responsible for the electrocardiographic phenotype of the Brugada syndrome are temperature dependent. Circ Res 1999;85:803–9.
20. Roden DM. Taking the "idio" out of "idiosyncratic": predicting Torsades de Pointes. Pacing Clin Electrophysiol 1998;21:1029–34.
21. Vos MA, Verduyn SC, Gorgels APM, et al. Reproducible induction of early afterdepolarizations and Torsade de Pointes arrhythmias by d-sotalol and pacing in dogs with chronic atrioventricular block. Circulation 1995;91:864–72.
22. Vos MA, Groot SHM, Verduyn SC, et al. Enhanced susceptibility for acquired Torsade de Pointes arrhythmias in the dog with chronic, complete AV block is related to cardiac hypertrophy and electrical remodeling. Circulation 1998;98:1125–35.
23. Volders PGA, Sipido KR, Vos MA, et al. Downregulation of delayed rectifier K^+ currents in dogs with chronic complete atrioventricular block and acquired Torsades de Pointes. Circulation 1999;100:2455–61.
24. Burashnikov A, Antzelevitch C. Prominent I_{Ks} in epicardium and endocardium contributes to development of transmural dispersion of repolarization but protects against development of early afterdepolarizations. J Cardiovasc Electrophysiol 2002;13:172–7.
25. Follmer CH, Colatsky TJ. Block of delayed rectifier potassium current, I_K, by flecainide and E-4031 in cat ventricular myocytes. Circulation 1990;82:289–93.
26. Martínez HB, Elizalde A, Chapula JS. Developmental differences in delayed rectifying outward current in feline ventricular myocytes. Am J Physiol 2000;278:H484–92.
27. January CT, Riddle JM. Early afterdepolarizations: mechanism of induction and block, a role for L-type Ca^{2+} current. Circ Res 1989;64:977–90.
28. Luo CH, Rudy Y. A dynamic model of the cardiac ventricular action potential II afterdepolarizations, triggered activity, and potentiation. Circ Res 1994;74:1097–113.
29. Bányász T, Fülöp L, Magyar J, et al. Endocardial versus epicardial differences in L-type calcium current in canine ventricular myocytes studied by action potential voltage clamp. Cardiovasc Res 2003;58: 66–75.
30. Cordeiro JM, Greene L, Heilmann C, Antzelevitch D, Antzelevitch C. Transmural heterogeneity of calcium activity and mechanical function in the canine left ventricle. Am J Physiol 2004;286:H1471–9.
31. Greenstein JL, Wu R, Po S, et al. Role of the calcium-independent transient outward current Ito1 in shaping action potential morphology and duration. Cir Res 2000;87:1026–33.
32. Miyoshi S, Mitamura H, Fujikawa K, et al. A mathematical model of phase 2 reentry: role of L-type Ca current. Am J Physiol 2003;284: H1285–94.
33. Furukawa T, Myerburg RJ, Furukawa N, et al. Differences in transient outward currents of feline endocardial and epicardial myocytes. Circ Res 1990;67:1287–91.
34. Zygmunt AC, Goodrow RJ, Antzelevitch C. I_{NaCa} contributes to electrical heterogeneity within the canine ventricle. Am J Physiol 2000;278:H1671–8.
35. Sanguinetti MC, Jurkiewicz NK, Scott A, Siegl PKS. Isoproterenol antagonizes prolongation of refractory period by class III antiarrhythmic agent E-4031 in guinea pig myocytes, mechanism of action. Circ Res 1991;68:77–84.
36. Kimura S, Bassett AL, Xi H, Myerburg RJ. Early afterdepolarizations and triggered activity induced by cocaine, a possible mechanism of cocaine arrhythmogenesis. Circulation 1992;85:2227–35.

Response of beat-by-beat QT variability to sympathetic stimulation in the LQT1 form of congenital long QT syndrome

Kazuhiro Satomi, MD,[a] Wataru Shimizu, MD, PhD,[a] Hiroshi Takaki, MD,[b] Kazuhiro Suyama, MD, PhD,[a] Takashi Kurita, MD, PhD,[a] Naohiko Aihara, MD,[a] Shiro Kamakura, MD, PhD[a]

[a]*From the Division of Cardiology, Department of Internal Medicine, and*
[b]*Department of Cardiovascular Dynamics, National Cardiovascular Center, Suita, Japan.*

OBJECTIVES The purpose of this study was to test the hypothesis that the lability of beat-by-beat QT variability is prominent during sympathetic stimulation in LQT1 patients. We analyzed beat-by-beat QT variability using a newly developed program and applied cross-correlation methods in LQT1 patients before and after epinephrine infusion.

BACKGROUND Studies suggest that cardiac events associated with sympathetic stimulation are more common in the LQT1 form than the LQT2 and LQT3 forms of congenital long QT syndrome (LQTS). Although beat-by-beat alternation of T-wave morphology is observed in LQTS, its objective estimation is difficult because of complicated T-wave morphology.

METHODS Twelve-lead ECG was recorded under baseline conditions and during epinephrine infusion (0.1 μg/kg/min) in 14 LQT1 and five control patients. We measured beat-by-beat QT interval by a cross-correlation technique. Mean of successive changes in RR (ΔRR), QT (ΔQT), standard deviation of ΔRR (SD-ΔRR), ΔQT (SD-ΔQT), and QTI (QT/ RR) before and after epinephrine were compared between the two groups.

RESULTS No significant differences in any parameters were observed between the two groups under baseline conditions. ΔQT, SD-ΔQT, and QTI were increased in LQT1 but not in control patients during epinephrine (LQT1: ΔQT 2.3–4.2 ms, SD-ΔQT 2.2–4.1, QTI 0.10–0.22, $P < .005$ vs baseline; Control: ΔQT 2.5–2.4 ms, SD-ΔQT 1.9–2.1, QTI 0.08–0.09: P = NS vs baseline).

CONCLUSIONS Beat-by-beat QT variability analyzed by the cross-correlation method was greater in LQT1 patients during epinephrine infusion, suggesting sympathetic stimulation accentuates beat-by-beat alternation of repolarization in LQT1 patients.

KEYWORDS Long QT syndrome; Epinephrine; Sympathetic activity; QT interval; T-wave alternans

(Heart Rhythm 2005;2:149–154)

Introduction

The congenital long QT syndrome (LQTS) is a hereditary disorder associated with prolonged ventricular repolarization and the life-threatening polymorphic ventricular tachycardia torsades de pointes (TdP).[1,2] Genetic studies have shown that congenital LQTS is a primary electrical disease caused by mutation in specific ion channel genes.[3,4] Seven forms of congenital LQTS have been identified.

Among the seven forms, cardiac events associated with sympathetic stimulation are more common in the LQT1 form than in the other forms of congenital LQTS.

T-wave alternans (TWA), an ECG phenomenon characterized by beat-by-beat alternation of the morphology, amplitude, and/or polarity of the T wave, often is associated with congenital LQTS. TWA is an important prognostic indicator because it is commonly observed just preceding episodes of TdP.[5–7] Although beat-by-beat alternation of repolarization somewhere in the heart is presumed to underlie TWA, its objective estimation is difficult because of complicated T-wave morphology.

The present study used a novel method "cross-correlation technique" to assess beat-by-beat QT variability. The aim of the study was to test the hypothesis that the lability

Dr. Shimizu was supported in part by the Vehicle Racing Commemorative Foundation; Ichiro Kanahara Foundation; Mochida Memorial Foundation for Medical and Pharmaceutical Research; Health Sciences Research Grants from the Ministry of Health, Labor, and Welfare; and Research Grants for Cardiovascular Diseases (15C-6) from the Ministry of Health, Labor and Welfare, Japan.

Address reprint requests and correspondence: Dr. Wataru Shimizu, Division of Cardiology, Department of Internal Medicine, National Cardiovascular Center, 5-7-1 Fujishiro-dai, Suita, Osaka, 565-8565, Japan.

E-mail address: wshimizu@hsp.ncvc.go.jp.

(Received July 21, 2004; accepted November 1, 2004.)

1547-5271/$ -see front matter doi:10.1016/j.hrthm.2004.11.010

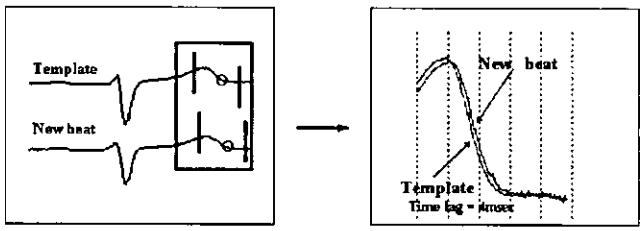

Figure 1 Algorithm of QT measurement by the cross-correlation method. See text for details.

of beat-by-beat QT variability is prominent during sympathetic stimulation in LQT1 patients in whom cardiac events often occur during sympathetic stimulation.

Methods

Study population

Fourteen LQT1 patients with *KCNQ1* mutation and five healthy volunteers used as controls were included in the study. The five healthy volunteers had no symptoms, and no abnormal T-wave morphologies were observed on 12-lead ECG. LQTS-affected individuals were noted based on the ECG diagnostic criteria of Keating et al.[8] The criteria include corrected QT (QTc) ≥470 ms in asymptomatic individuals and QTc >440 ms for men and >460 ms for women associated with one or more of the following: (1) stress-related syncope, (2) documented TdP, or (3) family history of early sudden cardiac death. Genotyping of LQTS was reviewed and approved by the Ethical Review Committee. Written informed consent was obtained from all patients.

Recording of standard 12-lead ECG

Standard 12-lead ECG was recorded using an FDX6521 (Fukuda Denshi Co., Tokyo, Japan) with the patient in the supine position without antiarrhythmic medications, including beta-blockers. ECG data were digitized using analog-to-digital converters at a sampling rate of 1,000 samples/second per channel.

ECG measurements

We measured QT interval beat by beat in the most stable lead to analyze T-wave morphology among precordial leads. The beat-by-beat changes of the QT interval were assessed during the latter half of T wave (Figure 1).

Specifically, the steps involved in analyzing a digitized ECG record included the following. (1) The operator selected a lead to analyze and the beginning and the end of the template T wave as an average of consecutive five beats. (2) The time of each R wave was identified using an automated peak detection algorithm. (3) For each of the other new beats, the time lags between the new beat and the template were calculated for comparison with the templates of QT morphology by a *cross-correlation method.* The templates were resampled as successive five beats before the newest analyzed beat.

We also analyzed beat-by-beat QT interval using a semi-automated digitizing program simultaneously. QT interval was defined as the time interval between QRS onset and the point at which the isoelectric line intersected a tangential line drawn at the maximal downslope of the T wave *(tangential method).*

Epinephrine administration

The epinephrine test was conducted as part of the clinical evaluation of LQTS.

A bolus injection of epinephrine 0.1 μg/kg was followed immediately by continuous infusion at 0.1 μg/kg/min. Twelve-lead ECG was recorded continuously during sinus rhythm under baseline conditions and usually for 5 minutes after start of epinephrine infusion. The effect of epinephrine on RR and QT intervals usually reached steady-state conditions 2 to 3 minutes after epinephrine was started. Epinephrine infusion for more than 5 minutes was avoided. ECG monitoring was continued for another 5 minutes after finishing epinephrine infusion to detect any occurrence of TdP. ECG data were collected under baseline conditions and at steady-state epinephrine effect 3 to 5 minutes after epinephrine was started.

Analyzed parameters

The following five ECG parameters were calculated from all RR and QT intervals recorded for 30 seconds during baseline conditions and at steady-state epinephrine conditions and then compared between the two groups (Figure 2): (1) ΔRR, the average of successive RR interval changes; (2) ΔQT, the average of successive QT interval changes; (3) SD-ΔRR, the standard deviation of RR interval; (4) SD-ΔQT, the standard deviation of the QT interval; and (5) QT index (QTI), the rate of change of QT interval

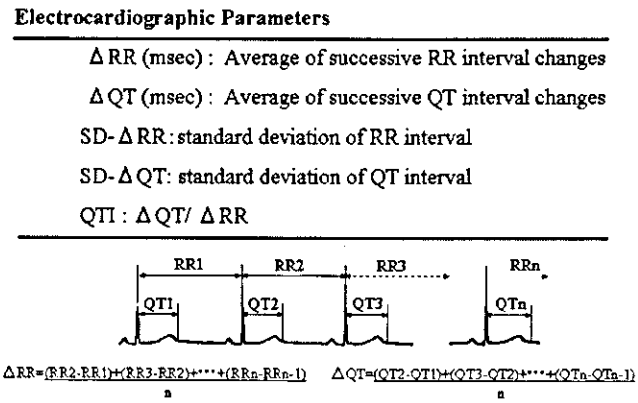

Figure 2 Five ECG parameters calculated in the present study. See text for details.

Table 1 Baseline ECG characteristics

	LQT1 (n = 14)	Control (n = 5)
Age	28 ± 20	29 ± 10
HR (bpm)	71 ± 10	68 ± 7
QT (ms)	454 ± 59*	387 ± 13
QTc (ms)	504 ± 76*	410 ± 36
$T_{peak\text{-}end}$ (ms)	102 ± 16	91 ± 19
QTD (ms)	71 ± 25*	45 ± 11

Values are reported as mean ± SD.
HR = heart rate; QTc = corrected QT interval; $T_{peak\text{-}end}$ = interval between T_{peak} and T_{end}; QTD = QT dispersion (maxQT-minQT).
*$P < .05$ vs control.

to RR interval, defined as the beat-by-beat value of ΔQT divided by ΔRR.

We examined the relationship between QT variability (ΔQT, SD-ΔQT) analyzed by cross-correlation methods and QT interval or heart rate before and after epinephrine infusion.

Statistical analysis

Data are expressed as mean ± SD. Paired and unpaired t-tests were used for couple observation. Correlation between continuous variables was tested by linear regression. For all tests, $P < .05$ was considered significant.

Results

Table 1 lists baseline ECG characteristics. No significant differences were observed regarding age and baseline heart rate between the LQT1 and control groups. The baseline QT and QTc intervals and QT dispersion, which were analyzed by the tangential method, were all significantly greater in the LQT1 group than in control group.

Beat-by-beat T wave variability before and after epinephrine

Figure 3 illustrates representative examples of superimposed QT complexes before and after epinephrine. The consecutive 10 beats of eight-lead ECGs were drawn temporally. In the control patient, no significant difference of beat-by-beat T-wave morphology was observed before and after epinephrine. In contrast, more significant beat-by-beat lability of the T wave was recognized after epinephrine in the LQT1 patient, although no significant change of beat-by-beat T-wave morphology was observed under baseline.

Beat-by-beat QT variability

The analyzed ECG leads were lead V_5 in three controls and six LQT1 patients, lead V_6 in two controls and five LQT1 patients, and lead V_2, V_3, and V_4 in each of the remaining LQT1 patients.

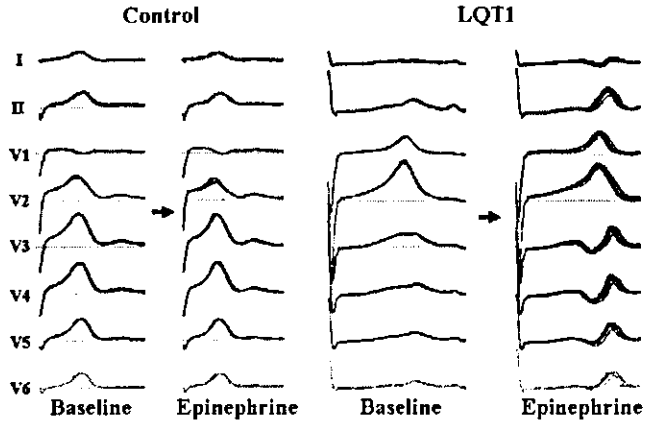

Figure 3 Representative example of superimposed QT complexes before and after epinephrine. The consecutive 10 beats of eight-lead ECGs are drawn temporally. In a control patient, no difference of beat-by-beat T-wave morphology is observed before and after epinephrine. However, more significant beat-by-beat alternans of T wave and change to biphasic T-wave pattern were observed after epinephrine in an LQT1 patient.

Figure 4 illustrates beat-by-beat change of the RR, QT, and the ΔRR and ΔQT in a control patient. The RR interval was decreased after bolus infusion of epinephrine, and remained decreased less than before epinephrine at the steady state condition. The ΔRR, which is heart rate variability, became small following the start of epinephrine. The QT interval was prolonged when the RR was decreased after bolus epinephrine, however the QT interval was slightly shortened compared before epinephrine at steady-state. The ΔQT was not changed before and after epinephrine infusion.

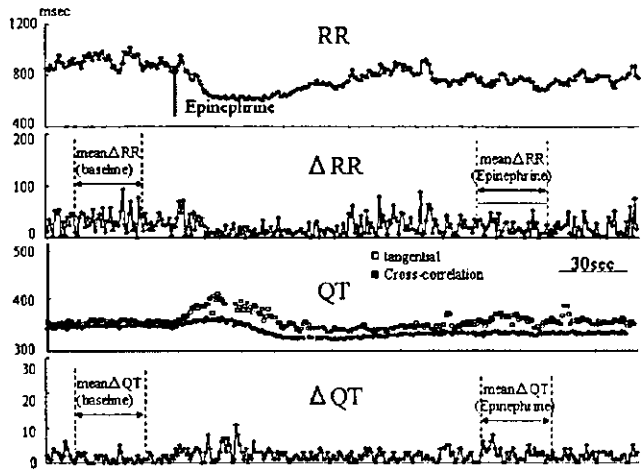

Figure 4 Beat-by-beat change of RR, QT, ΔRR, and ΔQT in a control patient. RR interval was decreased after bolus infusion of epinephrine and remained decreased less than before epinephrine at the steady-state condition. ΔRR became small after epinephrine was started. QT interval was prolonged when RR was decreased after bolus epinephrine but was slightly shortened compared with before epinephrine at the steady-state epinephrine effect. ΔQT was not changed before and after epinephrine infusion.

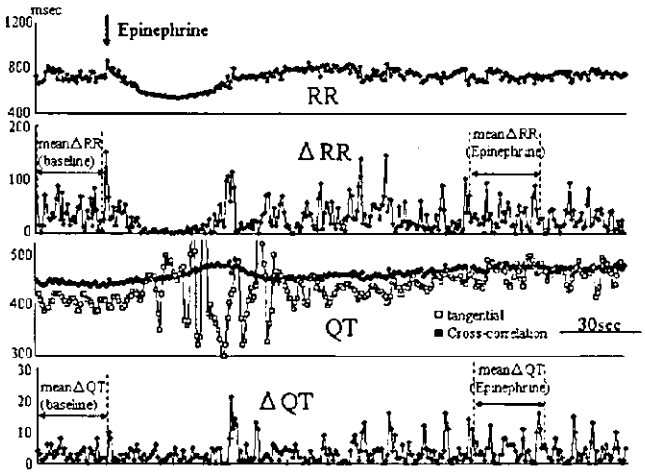

Figure 5 Beat-by-beat change of RR, QT, ΔRR, and ΔQT in an LQT1 patient. RR interval was decreased following bolus infusion of epinephrine and remained decreased at steady-state condition. ΔRR became small after bolus infusion of epinephrine. QT interval was prolonged after bolus infusion of epinephrine and remained prolonged at steady-state epinephrine effect compared with before epinephrine. Of note, ΔQT was significantly increased at steady-state epinephrine effect compared with before epinephrine.

Figure 5 illustrates beat-by-beat change of RR, QT, ΔRR, and ΔQT in an LQT1 patient. Similar to the control patient, the RR interval also was decreased following bolus infusion of epinephrine and remained decreased at steady-state epinephrine effect in the LQT1 patient. ΔRR became small after bolus infusion of epinephrine. QT interval was prolonged following the bolus infusion of epinephrine and remained prolonged at steady-state epinephrine effect compared before epinephrine. It is noteworthy that ΔQT was significantly increased at steady-state epinephrine effect compared with before epinephrine.

Table 2 lists composite data of the five ECG parameters before and at steady-state epinephrine effect in the LQT1 and control groups.

No significant differences in ΔRR, ΔQT, SD-ΔRR, SD-ΔQT, and QTI were observed between the two groups under baseline conditions. Epinephrine increased ΔQT (2.3 ± 0.3 to 4.2 ± 2.3 ms, $P < .005$), SD-ΔQT (2.2 ± 1.9 to 4.1 ± 2.2 ms, $P < .005$), and QTI (0.10 ± 0.06 to 0.22 ± 0.16, $P < .005$) in LQT1 group but not in control group (ΔQT 2.5 ± 1.5 to 2.4 ± 0.5 ms, SD-ΔQT 1.9 ± 0.9 to 2.1 ± 0.6 ms, QTI 0.08 ± 0.02 to 0.09 ± 0.06, P = NS) (Figure 6).

ΔQT and SD-ΔQT showed significant correlation with QTc after epinephrine (r = 0.61; $P < .05$ and r = 0.65; $P < .05$, respectively) but not before epinephrine. On the other hand, the values were not correlated with heart rate either before or after epinephrine. No significant differences in the five ECG parameters were observed between patients with (n = 8) and patients without (n = 6) a history of syncope or cardiac arrest.

Discussion

Quantification of ventricular repolarization

Several methods have been proposed to quantify abnormalities of repolarization[9,10]; however, few of the techniques are suitable for routine clinical use. Thus, assessment of ventricular repolarization still is based largely on QT and QTc measurements and on qualitative description of morphologic alterations such as presence of notched, bifid, or biphasic T waves. A set of new morphologic ECG parameters proposed by Merri et al,[11] Benhorin et al,[12] and Priori et al[13] could provide a better description of repolarization and be more reproducible than QT interval duration, but these parameters have not yet obtained widespread application in clinical practice.

RT interval, the duration between the peak of R and T wave, was used to analyze the repolarization period to minimize the observer bias in manual acquisition of data.[14] Experimental studies[15,16] using arterially perfused canine left ventricular wedges suggest both the peak and the end of the T wave on the ECG are coincident with repolarization of epicardial and maximal M-cell action potentials, respectively, so that the interval between the T_{peak} and T_{end} reflects transmural dispersion of repolarization. The transmural dispersion of repolarization, the latter part of the T wave, is linked to ventricular arrhythmias such as TdP under long QT conditions. Therefore, the RT interval cannot detect the

Table 2 ECG parameters before and after epinephrine in LQT1 and control groups

	LQT1 (n = 14)		Control (n = 5)	
	Baseline	Epinephrine	Baseline	Epinephrine
ΔRR	33 ± 28	36 ± 39	39 ± 20	34 ± 25
ΔQT	2.3 ± 0.3	4.2 ± 2.3*,†	2.5 ± 1.5	2.4 ± 0.5
SD-ΔRR	23 ± 18	27 ± 27	30 ± 17	36 ± 27
SD-ΔQT	2.2 ± 1.9	4.1 ± 2.2*,†	1.9 ± 0.9	2.1 ± 0.6
QTI	0.10 ± 0.06	0.22 ± 0.16*,†	0.08 ± 0.02	0.09 ± 0.06

Values are reported as mean ± SD.
*$P < .05$ vs baseline.
†$P < .05$ vs control.

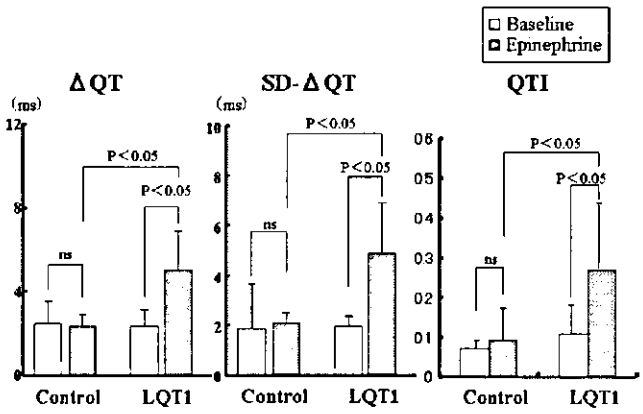

Figure 6 Comparison of ΔQT, SD-ΔQT, and QTI before and after epinephrine infusion between LQT1 and control groups. No significant differences in ΔQT, SD-ΔQT, and QTI were observed between the two groups under baseline conditions. Epinephrine increased ΔQT, SD-ΔQT, and QTI in the LQT1 group but not in the control group.

important part of the T wave and may underestimate a repolarization abnormality in patients with LQTS.

Our novel method, the cross-correlation method, analyzed beat-by-beat "time-lag" comparing the template of the latter part of the T wave, thus better description of QT interval could be assessed independently of complicated TU wave morphology. Beat-by-beat T-wave and QT variability measured by the cross-correlation method is not synonymous with T-wave alternans and could be analyzed more stably than with the standard tangential method even during epinephrine infusion in the two patient groups (Figures 4 and 5).

Variability of repolarization in LQT1 syndrome

Physical exercise and strong emotion precipitate syncope and sudden cardiac death in patients with congenital LQTS.[2] Experimental models[17,18] of LQTS and clinical studies[19] suggest catecholamine-enhanced early afterdepolarization and triggered activity play a pivotal role in the genesis of QT prolongation and TdP.

TWA is a well-known ECG phenomenon often associated with the development of cardiac arrhythmias,[20] particularly in the setting of acquired and congenital LQTS.[6,7] The phenomenon previously was described as QT interval variability or T-wave lability by the pronounced changes in T-wave morphology.[21,22] The mechanism underlying catecholamine-provoked T-wave lability is unclear. It also is clearly different from microvolt (μV-TWA). The μV-TWA shows no definite periodicity of the T-wave changes on surface ECG. Exercise-induced μV-TWA was not significantly different between genotype carriers and noncarriers in a study involving a large single kindred with LQTS.[21,23]

An experimental study by Shimizu and Antzelevitch[7] suggested that TWA observed at rapid rates under long QT conditions largely results from alternation of the M-cell action potential duration, leading to exaggeration of transmural dispersion of repolarization during alternating beats and thus the potential for development of TdP. Their data also suggested that unlike transient forms of TWA that damp out quickly and depend on electrical restitution factors, the steady-state electrical and mechanical alternans appears to largely result from beat-to-beat alternans of intracellular calcium cycling.

Our study showed that beat-by-beat QT variability was accentuated by epinephrine infusion only in LQT1 patients, indicating that variability of repolarization is made pronounced by sympathetic stimulation in patients of LQT1 but not in normal controls. Our result supports the clinical manifestation that life-threatening arrhythmia, such as TdP, often is observed under increased sympathetic activity in LQTS, especially in LQT1 patients.[23]

However, the numbers of families and individuals in the present study were small and limited the number of LQT1 patients. Therefore, our data may be limited to LQT1 and not applicable to LQTS patients with other genotypes.

Relationship among QT variability, QT interval, and heart rate

In the present study, QT variability after epinephrine was correlated with QTc interval after epinephrine but not with heart rate. The μV-TWA is a highly heart rate-dependent parameter and can be assessed invasively by arterial pacing or noninvasively by exercise. Heart rate threshold for induction of the μV-TWA was reported at 110 bpm in healthy adults.[24] No relationship between QT variability and heart rate after epinephrine was observed in this study, probably because of the lesser increase in heart rate in both groups.

Conclusion

Our data showed that beat-by-beat QT variability analyzed by the cross-correlation method was greater in LQT1 patients during sympathetic stimulation, suggesting that sympathetic stimulation accentuates beat-by-beat alternans of repolarization in the LQT1 syndrome.

References

1. Schwartz P, Malliani A. Electrical alterations of the T-wave: clinical and experimental evidence of its relationship with the sympathetic nervous system and with the long Q-T syndrome. Am Heart J 1975; 89:45–50.
2. Moss A, Schwartz P, Crampton R. The long QT syndrome: a prospective international study. Circulation 1985;71:17–21.
3. Vincent G. The molecular genetics of the long-QT syndrome: genes causing fainting and sudden death. Annu Rev Med 1998;49:263–74.
4. Priori S, Barhanin J, Hauer R. Genetic and molecular basis of cardiac arrhythmias: impact on clinical management, parts I and II. Circulation 1999;99:518–528.

5. Schwartz P, Priori S, Napolitano C. The Long QT Syndrome. Philadelphia: WB Saunders, 1999.
6. Shimizu W. T wave alternans: from cell to clinical. J Cardiovasc Electrophysiol 2001;12:428–430.
7. Shimizu W, Antzelevitch C. Cellular and ionic basis for T-wave alternans under long-QT conditions. Circulation 1999;99:1499–507.
8. Keating M, Atkinson D, Dunn C. Linkage of cardiac arrhythmia, the long QT syndrome, and the Harvey ras-1 gene. Science 1991;252: 704–705.
9. Bonatti V, Rolli A, Botti G. Recording of monophasic action potentials of the right ventricle in long QT syndromes complicated by severe ventricular arrhythmias. Eur Heart J 1983;4:168–179.
10. Mirvis D. Spatial variation of QT intervals in normal persons and patients with acute myocardial infarction. J Am Coll Cardiol 1989;5: 625–631.
11. Merri M, Benhorin J, Alberti M, Locati E, Moss A. Electrocardiographic quantitation of ventricular repolarization. Circulation 1989;80: 1301–1308.
12. Benhorin J, Merri M, Alberti M, Locati E, Moss A. Long QT syndrome: new electrocardiographic characteristics. Circulation 1990;82: 521–527.
13. Priori S, Mortara D, Napolitano C. Valuation of the spatial aspects of T-wave complexity in the long-QT syndrome. Circulation 1997;96: 3006–3012.
14. Krahn A, Klein G, R. Y. Hysteresis of the RT interval with exercise: a new marker for the long-QT syndrome? Circulation 1997;96:1551–1556.
15. Shimizu W, Antzelevitch C. Differential effects of beta-adrenergic agonists and antagonists in LQT1, LQT2 and LQT3 models of the long QT syndrome. J Am Coll Cardiol 2000;35:778–786.
16. Antzelevitch C, Shimizu W, Yan G. The M cell: its contribution to the ECG and to normal and abnormal electrical function of the heart. J Cardiovasc Electrophysiol 1999;10:1124–1152.
17. Shimizu W, Antzelevitch C. Cellular basis for the ECG features of the LQT1 form of the long-QT syndrome: effects of beta-adrenergic agonists and antagonists and sodium channel blockers on transmural dispersion of repolarization and torsade de pointes. Circulation 1998;98:2314–2322.
18. Priori S, Napolitano C, Cantu F. Diffrencial response to Na channel blockade β-adrenergic stimulation, and rapid pacing in a cellular model mimicking the SCN5A and HERG defect present in the long-QT syndrome. Circ Res 1996;78:1009–1015.
19. Shimizu W, Ohe T, Kurita T. Early after depolarizations induced by isoproterenol in patients with congenital long QT syndrome. Circulation 1991;84:1915–1923.
20. Smith J, Clancy E, Valeri C. Electrical alternans and cardiac electrical instability. Circulation 1988;77:110–121.
21. Nemec J, Hejlik J, Shen W, Ackerman M. Catecholamine-induced T-wave lability in congenital long QT syndrome: a novel phenomenon associated with syncope and cardiac arrest. Mayo Clin Proc 2003;78: 10–50.
22. Couderc J, Zareba W, Burattini L, Moss A. Beat-to-beat repolarization variability in LQTS patients with the SCN5A sodium channel gene mutation. Pacing Clin Electrophysiol 1999;22:1581–1592.
23. Kaufman E, Priori S, Napolitano C. Electrocardiographic prediction of abnormal genotype in congenital long QT syndrome: experience in 101 related family members. J Cardiovasc Electrophysiol 2001;12: 455–461.
24. Hohnloser S, Klingenheben T, Zabel M, Li Y, Albrecht P, Cohen R. T wave alternans during exercise and atrial pacing in humans. J Cardiovasc Electrophysiol 1997;8:987–993.

先天性QT延長症候群の遺伝子型と表現型

清水 渉*

abstract

先天性QT延長症候群は，QT時間の延長とtorsade de pointesを主徴とする遺伝性疾患である．現在までに8つの遺伝子型が報告されているが，特に頻度の多いLQT1，LQT2，LQT3では，遺伝子型と表現型との関連（genotype-phenotype correlation）が詳細に検討されており，循環器疾患の遺伝子診断における最先端の領域である．各遺伝子型により，特徴的な異常T波，交感神経刺激に対する反応性の違いに基づく心事故（失神発作，突然死）の誘因，重症度，自然経過，および予後が異なることから，患者の生活指導にこれらが反映され，また，各遺伝子型の細胞学的成因に基づいた遺伝子型特異的な治療法も実践されつつある．最近では，各原因遺伝子中の変異部位別の臨床病態の違いも報告され始めており，今後，ますます発展していく領域と考えられる．

I はじめに

先天性QT延長症候群（LQTS）は，多くの場合安静時からQT時間の延長を認め，おもに運動中などの交感神経緊張時にtorsade de pointes（TdP）と称される多形性心室頻拍が出現し，失神や突然死の原因となる遺伝性疾患である[1]．

1990年代からの分子生物学的研究の飛躍的な進歩により，先天性LQTSは，心筋イオンチャネル機能や細胞膜タンパクの調節に関係する遺伝子異常が原因であることが判明した．

現在では，先天性LQTSの50～70%の家系で原因遺伝子が同定され，遺伝子型と表現型との関連（genotype-phenotype correlation）が詳細に検討されている．

II 遺伝子型

1995年に最初の原因遺伝子が同定されて以来，過日Cell誌に報告されたLQT8[2]も含めRomano-Ward症候群では八つの遺伝子型が報告されている（表1）．

LQT1とLQT5は遅延整流K^+電流（I_K）の活性化の遅い成分（I_{Ks}）の機能低下（loss of function），LQT2とLQT6はI_Kの活性化の速い成分（I_{Kr}）の機能低下，LQT3はlate Na^+電流（I_{Na}）の機能亢進（gain of function），LQT4はNa^+/K^+ ATPaseやNa^+-Ca^{2+}交換系電流（$I_{Na.Ca}$）などの細胞膜タンパク発現に関係する*Ankyrin-B*の変異により細胞内Ca^{2+}負荷をきたし，いずれもQTが延長する．

症候の一つとしてQT延長を認めるものに，周期性四肢麻痺と骨格異常を合併するLQT7（Andersen症候群），先天性心奇形，合指症，免疫不全，自閉

* 国立循環器病センター心臓血管内科医長

タイプ	遺伝子座	原因遺伝子	イオンチャネル
Romano-Ward症候群			
LQT1	11(11p15.5)	*KCNQ1*	I_{Ks}
LQT2	7(7q35-36)	*KCNH2*	I_{Kr}
LQT3	3(3p21-24)	*SCN5A*	I_{Na}
LQT4	4(4q25-27)	*Ankyrin-B*	Na^+-K^+ ATPase, $I_{Na,Ca}$
LQT5	21(21q22.1-q22.2)	*KCNE1*	I_{Ks}
LQT6	21(21q22.1-q22.2)	*KCNE2*	I_{Kr}
LQT7	17(17q23)	*KCNJ2*	I_{K1}
LQT8	12(12p13.3)	*CACNA1C*	$I_{Ca,L}$
Jervell & Lange-Nielsen症候群			
JLN1	11(11p15.5)	*KCNQ1 (homozygous)*	I_{Ks}
JLN2	21(21q22.1-q22.2)	*KCNE1 (homozygous)*	I_{Ks}

表1
先天性QT延長症候群の原因遺伝子とイオンチャネル機能

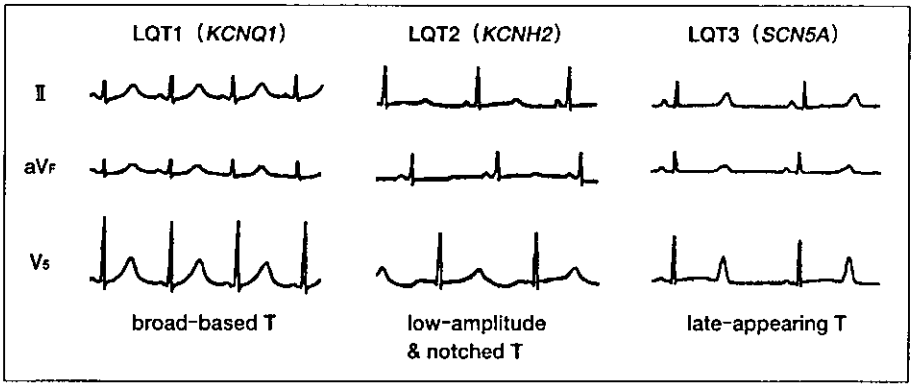

図1
先天性QT延長症候群の遺伝子型（LQT1, LQT2, LQT3）に特徴的な異常T波
LQT1では幅広い（broad-based）T波，LQT2ではノッチを伴う平低（low-amplitude, notched）T波，LQT3ではST部分の長い（late-appearing）T波が特徴的である．〔参考文献4)より引用改変〕

症などを合併するLQT8（Timothy症候群）がある．LQT7では内向き整流K^+電流（I_{K1}）の機能低下，LQT8ではL型Ca^{2+}電流（$I_{Ca,L}$）の機能亢進によりQT延長を認める．

両側性感音性難聴を伴うJervell&Lange-Nielsen症候群の一部の家系は，LQT1とLQT5の原因遺伝子である*KCNQ1*または*KCNE1*のホモ接合体であることが報告されている（JLN1とJLN2）[3]．

III 遺伝子型と表現型の関連

各遺伝子型の頻度は，LQT1が40%，LQT2が30～40%，LQT3が10%，LQT5とLQT6が2～5%，LQT4, LQT7, LQT8については報告例のみであり，遺伝子型と表現型（臨床所見）の関連は頻度の多いLQT1, LQT2, LQT3で主に検討されている．

1 異常T波

LQT1では幅広い（broad-based）T波，LQT2ではノッチを伴う平低（low-amplitude, notched）T波，LQT3ではST部分の長い（late-appearing）T波が特徴的とされている（図1）[4]．LQT4やLQT7ではTU波の異常を認め，とくにLQT7ではT波と分離した幅広く振幅の高いU波が特徴的であり，LQTSに含めるべきではないという意見もある．

LQT1, LQT2, LQT3の異常T波の成因には，心外膜細胞から心筋中層に存在する活動電位持続時間（APD）の長いmid-myocardial（M）細胞，さらに心内膜細胞にかけての貫壁性の活動電位プラトー相の電位勾配が関与すると考えられている[5,6]．

2 心事故の誘因

LQT1では心事故（失神発作，蘇生に成功した心停止，突然死）の62%は運動中に起こり，交感神経刺激に対して最も感受性が強い遺伝子型である[7]．また，水泳はLQT1に特異的な誘因であると報告されている．

LQT2では心事故の43%は，情動ストレス（恐怖や驚愕），睡眠中の雑音（目覚まし時計など）による覚醒時など，急激に交感神経が緊張する状態で起こり[8]，また出産前後の心事故はLQT2に特徴であ

ることも報告されている[9].

一方，LQT3では，心事故の多くは睡眠中や安静時に多いとされている．LQT4では運動後や精神的ストレス時に，LQT7では低K^+血症時に心事故が多いことが報告されている．

LQT1，LQT2，LQT3の心事故の誘因の違いは，交感神経刺激に対する反応性の違いによると考えられる．

各遺伝子型の患者にエピネフリン負荷試験（0.1 μg/kgボーラス静注＋0.1μg/kg/分持続点滴）を行うと[10]，LQT1ではエピネフリン開始直後にQTcが著明に延長し，持続点滴中の定常状態でもQTc延長が持続するのに対して，LQT2ではエピネフリン開始直後に一過性の著明なQTc延長を認めるが，定常状態ではQTcはコントロールレベル近くまで短縮する．

一方，LQT3ではエピネフリン開始直後のQTc延長は軽度で，定常状態でのQTcはコントロールレベル以下に短縮する．逆に，このQTcの経時的な反応の違いから，エピネフリン負荷試験やトレッドミル運動負荷試験による遺伝子型の推定も試みられている（図2）[10].

3 重症度と予後

LQT1の初回心事故の発症年齢はLQT2，LQT3に比べて若く，20歳以降の初回発症は比較的少ないとされている．さらに，初回心事故の発生年齢は女性に比べて男性で若く，とくにLQT1男性では全例15歳以下で発症するとされている[11]．生涯心事故発生率はLQT3に比べLQT1，LQT2で高いが，LQT3では致死率が高いことも報告されている[12].

最近では，LQT1，LQT2，LQT3について，遺伝子型，QTc時間，性別による心事故のリスク階層化も報告されている[13]．QTc≧500msのLQT1，LQT2とLQT3男性をhigh risk（≧50%）群，QTc＜500msのLQT2女性とLQT3およびQTc≧500msのLQT3女性をintermediate risk（30～49%）群，そして，QTc＜500msのLQT2男性とLQT1をlow risk（＜30%）群としている．

しかし，これらの階層化はあくまで一つの指針であり，個々の患者または家系で慎重に経過観察をする必要がある．

4 遺伝子型特異的治療

LQT1は交感神経刺激に対して最も感受性の強い遺伝子型であり，運動制限とともにβ遮断薬の有効性が高く，国際登録によれば81%の患者で発作が抑制されるとされている[7]．水泳中の心事故が多いことから，とくに未成年者では競泳，潜水などは禁止する必要がある．

補助的抗不整脈薬として，late I_{Na}遮断作用をもつメキシレチンは，LQT1やLQT2ではQT短縮作用は軽度であるが，M細胞APDを選択的に短縮させて，貫壁性再分極時間の不均一性を減少させ[5]，有効性が期待できる．Ca^{2+}拮抗薬のベラパミルも，内向き電流を減少させることによりQT時間やAPDを短縮し，β遮断薬との併用で補助的効果が期待さ

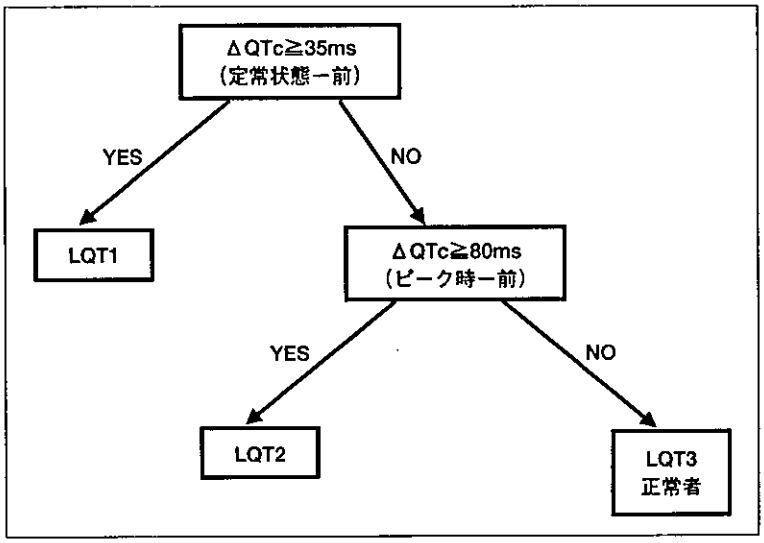

図2
エピネフリン負荷試験による遺伝子型の推定
エピネフリン負荷試験の定常状態で，修正QT（QTc）時間が35ms以上延長する場合にはLQT1と推定される．定常状態でのQTc延長が35ms未満で，かつエピネフリン負荷開始直後（ピーク時）のQTc延長が80ms以上の場合にはLQT2と推測される．それ以外の場合にはLQT3または正常者と考えられる．
〔参考文献10)より引用改変〕

れる[14].

$I_{K.ATP}$開口薬のニコランジルは，LQT1とLQT2において臨床的および実験的に有効性が報告されているが，有効血中濃度を考慮すると静注薬で補助的効果が期待される程度である[15), 16].

LQT2でも運動制限とともに第一選択薬はβ遮断薬であるが，LQT1に比べて有効率が低く（59%)[7]，ほかの抗不整脈薬（メキシレチン，ベラパミル）の併用が必要な場合が多い．また，LQT2患者では，K^+製剤とK^+保持性利尿薬の併用による血清K^+値の上昇により，QT時間が有意に短縮することが報告されている[17].

LQT3ではlate I_{Na}の機能亢進が原因であることから，これを遮断するメキシレチンによりQT時間は著明に短縮し，第一選択薬と考えられる[7]．動物実験の成績からβ遮断薬の効果はあまり期待できないが，LQT3患者数が少ないことから臨床的なエビデンスに乏しく，メキシレチンの有効性も含めて慎重に対応する必要がある．

一方でLQT3では，臨床的にも実験的にも，心拍数の増加によってQT時間が著明に短縮することから[5]，とくに徐脈例でペースメーカー治療が有効である．

β遮断薬を中心とする抗不整脈薬内服にもかかわらず再発を認める例，または心停止既往例では，いずれの遺伝子型でも植込み型除細動器の適応となる[18].

Ⅳ 今後の展望

遺伝性不整脈疾患のなかでも先天性LQTSは，循環器疾患の遺伝子診断における最先端の領域であり，遺伝子型と表現型との関連がもっとも詳細に検討されている．遺伝子型が判明することにより，より理論的な生活指導，治療が可能となり，もはや研究的な側面は少なく，近い将来保険適用になると思われる診断法である．

さらに，最近では遺伝子型にとどまらず，各原因遺伝子中の変異部位別の臨床病態の違いも報告され始めており[19), 20]，今後ますます発展していく領域と考えられる．

参考文献

1) Schwartz PJ, Moss AJ, Vincent GM, et al : Diagnostic criteria for the long QT syndrome. An update. Circulation 88 : 782～784, 1993
2) Splawski I, Timothy KW, Sharpe LM, et al : Ca (V) 1.2 calcium channel dysfunction causes a multisystem disorder including arrhythmia and autism. Cell 119 : 19～31, 2004
3) Splawski I, Timothy KW, Vincent GM, et al : Molecular basis of the long-QT syndrome associated with deafness. N Engl J Med 336 : 1562～1567, 1997
4) Moss AJ, Zareba W, Benhorin J, et al : ECG T-wave patterns in genetically distinct forms of the hereditary long QT syndrome. Circulation 92 : 2929～2934, 1995
5) Shimizu W, Antzelevitch C : Sodium channel block with mexiletine is effective in reducing dispersion of repolarization and preventing torsade de pointes in LQT2 and LQT3 models of the long-QT syndrome. Circulation 96 : 2038～2047, 1997
6) Shimizu W, Antzelevitch C : Cellular basis for the electrocardiographic features of the LQT1 form of the long QT syndrome. Effects of β adrenergic agonists, antagonists and sodium channel blockers on transmural dispersion of repolarization and torsade de pointes. Circulation 98 : 2314～2322, 1998
7) Schwartz PJ, Priori SG, Spazzolini C, et al : Genotype-phenotype correlation in the long-QT syndrome : gene-specific triggers for life-threatening arrhythmias. Circulation 103 : 89～95, 2001
8) Wilde AAM, Jongbloed RJE, Doevendans PA, et al : Auditory stimuli as a trigger for arrhythmic events differentiate HERG-related (LQT2) patients from KVLQT1-related patients (LQT1). J Am Coll Cardiol 33 : 327～332, 1999
9) Khositseth A, Tester DJ, Will ML, et al : Identification of a common genetic substrate underlying postpartum cardiac events in congenital long QT syndrome. Heart Rhythm 1 : 60～64, 2004
10) Shimizu W, Noda T, Takaki H, et al : Diagnostic value of epinephrine test for genotyping LQT1, LQT2 and LQT3 forms of congenital long QT syndrome. Heart Rhythm 1 : 276～283, 2004
11) Locati EH, Zareba W, Moss AJ, et al : Age- and sex-related differences in clinical manifestations in patients with congenital long-QT syndrome : findings from the international LQTS registry. Circulation 97 : 2237～2244, 1998
12) Zareba W, Moss AJ, Schwartz PJ, et al : Influence of the genotype on the clinical course of the long-QT syndrome. N Engl J Med 339 : 960～965, 1998
13) Priori SG, Schwartz PJ, Napolitano C, et al : Risk stratification in the long-QT syndrome. N Engl J Med 348 : 1866～1874, 2003
14) Aiba T, Shimizu W, Inagaki M, et al : Cellular and ionic mechanism for drug-induced long-QT syndrome and effectiveness of verapamil. J Am Coll Cardiol 45 : 300～307, 2005
15) Shimizu W, Kurita T, Matsuo K, et al : Improvement of repolarization abnormalities by a K^+ channel opener in the LQT1 form of congenital long QT syndrome. Circulation 97 : 1581～1588, 1998
16) Shimizu W, Antzelevitch C : Effects of a K^+ channel opener to reduce transmural dispersion of repolarization and prevent

torsade de pointes in LQT1, LQT2 and LQT3 models of the long-QT syndrome. Circulation 102 : 706～712, 2000
17) Etheridge SP, Compton SJ, Tristani-Firouzi M, et al : A new oral therapy for long QT syndrome : long-term oral potassium improves repolarization in patients with HERG mutations. J Am Coll Cardiol 42 : 1777～1782, 2003
18) Zareba W, Moss AJ, Daubert JP, et al : Implantable cardioverter defibrillator in high-risk long QT syndrome patients. J Cardiovasc Electrophysiol 14 : 337～341, 2003
19) Moss AJ, Zareba W, Kaufman ES, et al : Increased risk of arrhythmic events in long-QT syndrome with mutations in the pore region of the human ether-a-go-go-related gene potassium channel. Circulation 105 : 794～799, 2002
20) Shimizu W, Horie M, Ohno S, et al : Mutation site-specific differences in arrhythmic risk and sensitivity to sympathetic stimulation in the LQT1 form of congenital long QT syndrome : multi center study in Japan. J Am Coll Cardiol 44 : 117～125, 2004